ACADEMIC PRESS

Available online at www.sciencedirect.com

SCIENCE DIRECT®

Journal of Sound and Vibration 260 (2003) 213–235

JOURNAL OF SOUND AND VIBRATION

www.elsevier.com/locate/jsvi

Self-powered active vibration control using a single electric actuator

Kimihiko Nakano[a,*], Yoshihiro Suda[b], Shigeyuki Nakadai[c]

[a] *Department of Mechanical Engineering, Faculty of Engineering, Yamaguchi University. 2-16-1 Tokiwadai, Ube, Yamaguchi 755-8611, Japan*

[b] *Institute of Industrial Science, University of Tokyo, Tokyo, Japan*

[c] *Department of Mechanical Engineering, Chiba Institute of Technology, Chiba, Japan*

Received 11 September 2001; accepted 19 April 2002

Abstract

The authors have proposed self-powered active vibration control systems that achieve active vibration control using regenerated vibration energy. Such systems do not require external energy to produce a control force. This paper presents a self-powered system in which a single actuator realizes active control and energy regeneration.

The system proposed needs to regenerate more energy than it consumes. To discuss the feasibility of this system, the authors proposed a method to calculate the balance between regenerated and consumed energies, using the dynamical property of the system, the feedback gain of the active controller, the specifications of the actuator, and the power spectral density of disturbance. A trade-off was found between the performance of the active controller and the energy balance. The feedback gain of the active controller is designed to have good suppression performance under conditions where regenerated energy exceeds consumed energy.

A practical system to achieve self-powered active vibration control is proposed. In the system, the actuator is connected to the condenser through relay switches, which decide the direction of the electric current, and a variable resistor, which controls the amount of the electric current. Performance of the self-powered active vibration was examined in experiments; the results showed that the proposed system can produce the desired control force with regenerated energy, and that it had a suppression performance similar to that of an active control system using external energy. It was found that self-powered active control is attainable under conditions obtained through energy balance analysis.

*Corresponding author. Tel.: +81-836-85-9143; fax: +81-836-85-9101.
E-mail address: knakano@yamaguchi-u.ac.jp (K. Nakano).

0022-460X/03/$ - see front matter © 2002 Elsevier Science Ltd. All rights reserved.
PII: S0022-460X(02)00980-X

1. Introduction

Active vibration control has recently been applied to several vibration isolation devices [1]. Isolation performance has been better than that with passive control systems, but external energy, which is not consumed by typical passive systems, is required. This is one of the drawbacks of an active vibration control system. However, vibrating systems accumulate energy in the form of elastic potential energy or kinetic energy, and while a decrement of vibration means dissipation of a not small amount of energy; energy that in practice is not used at all. For example, simulation results have indicated that the dissipated energy of four dampers of a passenger car traversing a poor roadway at 13.4 m/s reached approximately 200 W of power [2,3].

One of the authors has proposed a system that achieves active vibration control using energy absorbed by dampers [4,5]. By utilizing linear DC motors, the authors realized a system, called a self-powered active vibration control system, which achieved active vibration control with only the regenerated energy [6,7]. In this system, the motor, called an energy regenerative damper, regenerates vibration energy and stores it in the condenser. Another motor achieves active vibration control using the stored energy. This system has already been applied to truck suspension systems [8].

Several papers have presented regenerative systems [9–14]. Wendel and Stecklein [9] proposed regenerative systems in automobile suspensions, and discussed possible configurations. Saito et al. [10] converted vibration energy to electric energy and accumulated it in a condenser. Harada et al. [11] utilized a linear DC motor as a damper, which regenerated vibration energy. Kim and Okada [12] improved efficiency of regeneration by using a pulse width modulated (PWM) step-up chopper. Noritsugu et al [13] proposed to regenerate vibration energy by a pneumatic actuator for automobile suspensions. Jolly and Margolis [14] proposed a regenerative vibration control system with a pneumatic actuator. In these studies, the potential performances of the regenerative systems and their applications to practical systems were discussed.

This paper proposes a new system that realizes self-powered active vibration control with a single linear DC motor. In this system, the motor produces a control force with regenerating vibration energy. The objectives of this study were:

(1) to predict the amount of energy required for active control and to obtain the conditions under which the proposed system would be feasible.
(2) to design an active controller based on energy balance analysis.
(3) to propose an electric circuit for a motor that could achieve energy regeneration and active control.
(4) to realize the proposed system and to examine the performance of this system through experiments.

2. Schematic view of the proposed system

A new system that realizes self-powered active vibration control with a single electric motor is proposed. This paper applies it to a two-degree-of-freedom active suspension. An electric motor is installed in the secondary suspension and produces the control force. The motor generates power when the speed of the armature is high. In this mode, the motor acts as a generator and simulates

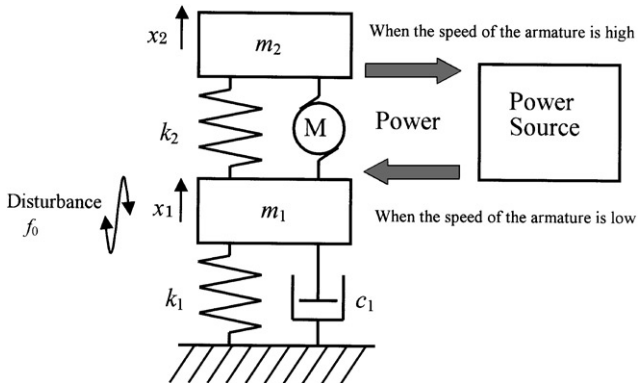

Fig. 1. Concept of the proposed system.

the desired output force with the reaction force of the armature. However, a typical motor system dissipates the generated power in the resistance of the electric circuits, since the power source of the motor cannot regenerate it. The authors propose a system that regenerates this energy. The regenerated energy is utilized when the speed of the armature is low and the motor cannot generate energy. When the motor generates more energy than it consumes, self-powered active control is attainable. Fig. 1 shows the concept of the proposed system. To examine the feasibility of the proposed system, the power consumption in active control systems is analyzed.

3. Power consumption in active control systems

3.1. Motion equations

The following equations depict motion equations of a two-degree-of-freedom suspension model as shown in Fig. 1. The electric actuator, installed in the system, produces control input f to reduce vibration of the second mass m_2. The equations of motions are represented as follows:

$$\ddot{x}_2 + \omega_2^2(x_2 - x_1) = \frac{f}{m_2}, \tag{1}$$

$$\ddot{x}_1 + 2\omega_1\varsigma_1\dot{x}_1 + \omega_1^2 x_1 = \frac{m_2}{m_1}\omega_2^2(x_2 - x_1) + \frac{f_0}{m_1} - \frac{f}{m_1}, \tag{2}$$

where

$$\omega_1 = \sqrt{\frac{k_1}{m_1}}, \tag{3}$$

$$\omega_2 = \sqrt{\frac{k_2}{m_2}}, \tag{4}$$

$$\varsigma_1 = \frac{c_1}{2\sqrt{k_1 m_1}}, \tag{5}$$

3.2. Model of an actuator

A linear DC motor is utilized as the actuator in the active control system. When the stroke velocity of the linear motor is $\dot{z}$, induced voltage is e_i, electric current of the armature is i, and the motor force is f, the following equations depict the relationship in linear DC motors:

$$e_i = -\varphi \dot{z}, \tag{6}$$

$$f = \varphi i. \tag{7}$$

The proportionality constant φ is called the motor constant. Force is produced when the armature of the motor, whose terminals are connected to each other, moves. It is obtained as

$$f = -\frac{\varphi^2}{r}\dot{z}, \tag{8}$$

where r is resistance of the armature.

Eq. (8) indicates that the motor acts as a viscous damper. The damping coefficient of the motor is called an equivalent damping coefficient and is symbolized by c_{eq}. It is defined as

$$c_{eq} = \frac{\varphi^2}{r}. \tag{9}$$

The equivalent damping ratio is defined as the ratio of the equivalent damping coefficient to the critical damping coefficient. It is written as

$$\varsigma_{eq} = \frac{c_{eq}}{2\sqrt{m_2 k_2}}. \tag{10}$$

3.3. Active controller

The active controller decides the desirable force of the actuator. It is designed on the basis of a skyhook control scheme [15,16], in which the desired actuator force is derived by

$$f^* = -c_{sky}\dot{x}_2, \tag{11}$$

where c_{sky} is the feedback gain of the controller. In the skyhook control system, the actuator produces a damping force proportional to the absolute velocity of the controlled mass, while a typical viscous damper generates a damping force proportional to its relative velocity. This improves the system's suppression performance. The ratio of the feedback gain to the critical damping coefficient is symbolized by ζ_{sky}. This is defined as

$$\varsigma_{sky} = \frac{c_{sky}}{2\sqrt{m_2 k_2}} \tag{12}$$

and is called the feedback gain ratio.

Fig. 2 shows the frequency response of the second mass displacement from the disturbance f_0. Values of the parameters are shown in Table 1. Note that m_1 and ω_1 equal m_2 and ω_2,

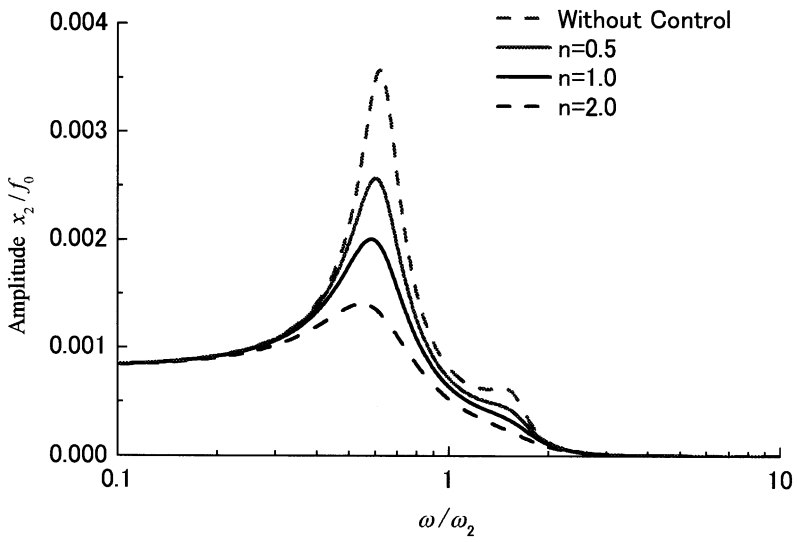

Fig. 2. Frequency response of the displacement of the second mass with skyhook control.

respectively. This makes the model simple and we can clearly see the characteristics of the proposed system. In the figure, n represents the ratio of the feedback gain to the equivalent damping coefficient of the actuator. This is a non-dimensional feedback gain. The following equation depicts the definition of n:

$$n = \frac{c_{sky}}{c_{eq}}. \tag{13}$$

The response of the system without control is also shown. The isolation performance becomes better as the feedback gain ratio becomes higher.

3.4. Power flow in electric actuator

When voltage of the power source is e_p, output of the actuator is

$$f = \varphi\frac{e_p - \varphi\dot{z}}{r} \tag{14}$$

To obtain the desired force, f^*, the following voltage is required:

$$e_p = \frac{r}{\varphi}f^* + \varphi\dot{z}. \tag{15}$$

Then current of the armature is

$$i = \frac{f^*}{\varphi}. \tag{16}$$

When the actuator produces the desired force, the power source consumes the power, E_c, which is described as

$$E_c = e_p i = \frac{1}{c_{eq}}f^2 + f\dot{z}. \tag{17}$$

Table 1
Specifications of the model

Description	Symbol	Value
Mass	m_1, m_2	1.6 kg
Angular natural frequency	ω_1, ω_2	27.6 rad/s
Damping ratio	ζ	0.3
Motor constant	φ	9.8 N/A
Resistance	r	4.7 Ω

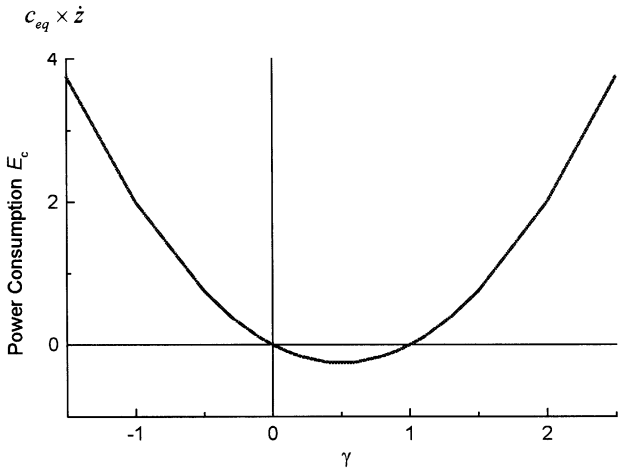

Fig. 3. Correlation between the mode variable and power consumption.

When $\dot{z} \neq 0$, we define γ as

$$\gamma = \frac{f}{-c_{eq}\dot{z}}. \tag{18}$$

This is called the "mode variable". To simplify the example, we neglect the case of $\dot{z} = 0$. The power consumption is derived as

$$E_c = c_{eq}\dot{z}^2\gamma(\gamma - 1). \tag{19}$$

The power consumption is allowed to be negative. When the power consumption takes a negative value the power source regenerates energy. Fig. 3 shows the correlation between γ and E_c. According to the value of γ, the characteristic of the actuator changes [17,18].

To understand the power flow in the actuator, we introduce the power output of the actuator, M_c, which is defined as

$$M_c = f\dot{z} = -c_{eq}\dot{z}^2\gamma. \tag{20}$$

When $0 < \gamma < 1$, both M_c and E_c become negative. This indicates that the actuator accepts energy from the suspension and delivers it to the power source. The actuator acts as a generator and regenerates vibration energy. This mode is labelled as "regeneration mode".

When $\gamma \leqslant 0$, both of M_c and E_c are greater than or equal to zero. The actuator transfers the energy to the suspension from the power source. This mode is called "drive mode".

When $\gamma \geqslant 1$, E_c is greater than or equal to zero, while M_c is less than or equal to zero. The actuator accepts energy from the suspension and the power source. Then the energy is dissipated in the resistance of the armature. The actuator produces a large damping force with energy supplied by the power source. This mode is called "brake mode".

When the system regenerates energy in the regeneration mode and uses it in the drive or brake modes, it can achieve active vibration control without external energy. In this way, one actuator achieves self-powered active control.

4. Analysis of energy balance

4.1. Average power consumption

When the power source accepts more energy than it releases, the average electric power consumption becomes negative. This, then, is the necessary condition for the proposed self-powered active vibration control system. Estimating the average power consumption is called energy balance analysis, and this needed to be conducted before we could design the active controller. The average power consumption $\bar{E}_c$ is obtained from Eq. (21).

$$\bar{E}_c = \lim_{\tau \to \infty} \frac{1}{\tau} \int_0^\tau \left(\frac{1}{c_{eq}} f^2 + f\dot{z} \right) \mathrm{d}t. \tag{21}$$

It is expressed as

$$\bar{E}_c = \frac{1}{\pi} \int_0^\infty \varepsilon_c(\omega) P_0(\omega)\, \mathrm{d}\omega, \tag{22}$$

where

$$\varepsilon_c(\omega) = \frac{1}{c_{eq}} |G_f(\mathrm{j}\omega)|^2 + |G_f(\mathrm{j}\omega)||G_{\dot{z}}(\mathrm{j}\omega)| \cos(\Phi_f(\omega) - \Phi_{\dot{z}}(\omega)). \tag{23}$$

In this paper, G_i and Φ_i represent the transfer function and the phase angle of i, respectively. Power spectral density of the disturbance is symbolized by $P_0(\omega)$.

4.2. Characteristics of power consumption

When $m_1 = m_2$ and $\omega_1 = \omega_2$, $G_f(\mathrm{j}\omega)$ and $G_{\dot{z}}(\mathrm{j}\omega)$ of the two-degree-of-freedom suspension system under skyhook control are obtained by

$$G_f(\mathrm{j}\omega) = -2 \cdot \varsigma_{sky} \cdot \frac{\mathrm{j}\omega'}{[(1-\omega'^2)^2 - \omega'^2 - 4\omega'^2 \varsigma_{sky}\varsigma_1] + \mathrm{j}2\omega'(1-\omega'^2)(\varsigma_{sky} + \varsigma_1)}, \tag{24}$$

$$G_{\dot{z}}(\mathrm{j}\omega) = \frac{1}{m_2\omega_2} \frac{-\omega'^2 \varsigma_{sky} + \mathrm{j}(\omega' - \omega'^3)}{[(1-\omega'^2)^2 - \omega'^2 - 4\omega'^2 \varsigma_{sky}\varsigma_1] + \mathrm{j}2\omega'(1-\omega'^2)(\varsigma_{sky} + \varsigma_1)}, \tag{25}$$

$$\Phi_f(\omega) = \tan^{-1}\frac{\mathrm{Im}(G_f(\mathrm{j}\omega))}{\mathrm{Re}(G_f(\mathrm{j}\omega))}, \tag{26}$$

$$\Phi_{\dot{z}}(\omega) = \tan^{-1}\frac{\mathrm{Im}(G_{\dot{z}}(\mathrm{j}\omega))}{\mathrm{Re}(G_{\dot{z}}(\mathrm{j}\omega))}, \tag{27}$$

where

$$\omega' = \frac{\omega}{\omega_2}. \tag{28}$$

Then

$$\varepsilon_c(\omega) = \frac{2\varsigma_{sky}}{m_2\omega_2}\left\{\frac{(n-\omega'^2)\omega'^2}{[(1-\omega'^2)^2-(\mu+4\varsigma_1\varsigma_{sky})\omega'^2]^2+4\omega'^2(1-\omega'^2)^2(\varsigma_{sky}+\varsigma_1)^2}\right\}. \tag{29}$$

Fig. 4 represents the relationship between ω' and $\varepsilon_c(\omega)$ when $n = 0.5, 1.0$ or 2.0. From Eq. (29) and Fig. 4, we can see that $\varepsilon_c(\omega)$ is less than zero when ω' is greater than $\sqrt{n}$.

From Eq. (22), the average power consumption is obtained by

$$\bar{E}_c = \frac{2\varsigma_{sky}}{\pi m_2}. \int_0^\infty \left\{\frac{(n-\omega'^2)\omega'^2}{[(1-\omega'^2)^2-(\mu+4\varsigma_1\varsigma_{sky})\omega'^2]^2+4\cdot\omega'^2(1-\omega'^2)^2(\varsigma_{sky}+\varsigma_1)^2}\right\} P_0(\omega')\,\mathrm{d}\omega'. \tag{30}$$

Assuming that disturbance is white noise, which contains a constant spectral density over all the frequency range, then the average power consumption is obtained from the integral of $\varepsilon_c(\omega)$ with respect to angular frequency. When $P_0(\omega') = 1$, the average power consumption is

$$\bar{E}_c = \frac{2\varsigma_{sky}}{\pi m_2}. \int_0^\infty \left\{\frac{(n-\omega'^2)\omega'^2}{[(1-\omega'^2)^2-(\mu+4\varsigma_1\varsigma_{sky})\omega'^2]^2+4\omega'^2(1-\omega'^2)^2(\varsigma_{sky}+\varsigma_1)^2}\right\} \mathrm{d}\omega'. \tag{31}$$

Then we define q as

$$q = \ln\omega'. \tag{32}$$

By substituting ω' for e^q, we obtain

$$\bar{E}_c = \frac{2\varsigma_{sky}}{\pi m_2}. \int_{-\infty}^\infty \left\{\frac{(n-\mathrm{e}^{2q})\mathrm{e}^{2q}}{[(1-\mathrm{e}^{2q})^2-(\mu+4\varsigma_1\varsigma_{sky})\mathrm{e}^{2q}]^2+4\mathrm{e}^{2q}(1-\mathrm{e}^{2q})^2(\varsigma_{sky}+\varsigma_1)^2}\right\} \mathrm{e}^q\,\mathrm{d}q. \tag{33}$$

We define the function $Q(q)$ as

$$Q(q) = \frac{(n-\mathrm{e}^{2q})\mathrm{e}^{2q}}{[(1-\mathrm{e}^{2q})^2-(\mu+4\varsigma_1\varsigma_{sky})\mathrm{e}^{2q}]^2+4\mathrm{e}^{2q}(1-\mathrm{e}^{2q})^2(\varsigma_{sky}+\varsigma_1)^2}\mathrm{e}^q. \tag{34}$$

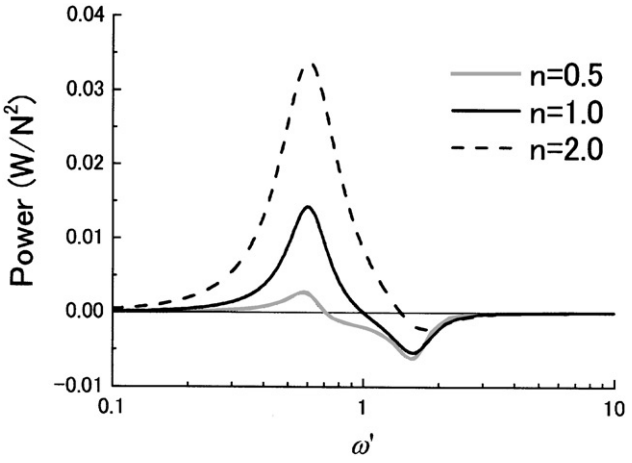

Fig. 4. Relationship between ω' and $\varepsilon_c(\omega)$ when $n = 0.5$, 1.0 or 2.0.

The average power consumption is written as

$$\bar{E}_c = \frac{2\varsigma_{sky}}{\pi m_2} \int_{-\infty}^{\infty} Q(q)\,\mathrm{d}q \tag{35}$$

From Eq. (34), we obtain

$$\begin{aligned} Q(-q) &= \frac{(n - \mathrm{e}^{-2q})\mathrm{e}^{-2q}}{[(1-\mathrm{e}^{-2q})^2 - (\mu + 4\varsigma_1\varsigma_{sky})\mathrm{e}^{-2q}]^2 + 4\mathrm{e}^{-2q}(1-\mathrm{e}^{-2q})^2(\varsigma_{sky}+\varsigma_1)^2}\mathrm{e}^{-q} \\ &= \frac{(n\mathrm{e}^{2q} - 1)\mathrm{e}^{2q}}{[(1-\mathrm{e}^{2q})^2 - (\mu + 4\varsigma_1\varsigma_{sky})\mathrm{e}^{2q}]^2 + 4\mathrm{e}^{2q}(1-\mathrm{e}^{2q})^2(\varsigma_{sky}+\varsigma_1)^2}\mathrm{e}^{q}. \end{aligned} \tag{36}$$

Then

$$Q(q) + Q(-q) = \frac{(n-1)(\mathrm{e}^{2q} + \mathrm{e}^{4q})}{[(1-\mathrm{e}^{2q})^2 - (\mu + 4\varsigma_1\varsigma_{sky})\mathrm{e}^{2q}]^2 + 4\mathrm{e}^{2q}(1-e^{2q})^2(\varsigma_{sky}+\varsigma_1)^2}\mathrm{e}^{q}. \tag{37}$$

From Eq. (37), we find the following relations:

$$Q(q) + Q(-q) > 0 \quad (n > 1), \tag{38}$$

$$Q(q) + Q(-q) = 0 \quad (n = 1), \tag{39}$$

$$Q(q) + Q(-q) < 0 \quad (n < 1). \tag{40}$$

Then the average consumption becomes

$$\bar{E}_c > 0 \quad (n > 1), \tag{41}$$

$$\bar{E}_c = 0 \quad (n = 1), \tag{42}$$

$$\bar{E}_c < 0 \quad (n < 1), \tag{43}$$

For example, when $n = 2.0$, 1.0 and 0.5 $\bar{E}_c$ becomes 0.12, 0.0 and $-0.04\,\mathrm{W/N^2}$ respectively. These results follow the theoretical analysis. The average power consumption, the energy balance analysis, represents energy balance between charged and discharged energies.

4.3. Experiments to measure energy balance

Experiments were carried out to measure energy balance. Fig. 5 shows a schematic view of the experimental two-degree-of-freedom suspension system set-up. The secondary suspension contains a linear DC motor, which acts as an actuator. The linear DC motor under the basement produces vibration. Two laser displacement sensors measure the displacement of each mass. The electric current of the armature and the supplied voltage are measured. These measured data are transmitted to a personal computer through the analog digital converter. The computer calculates the desired control force and sends the signal to the power source through a digital analog converter. Then the motor produces the control force. The specifications of the experimental set-up are the same as those in Table 1.

Power consumption when the system was subjected to a sinusoidal force was measured as the product of the current in the armature and the voltage of the power source. Dividing the power

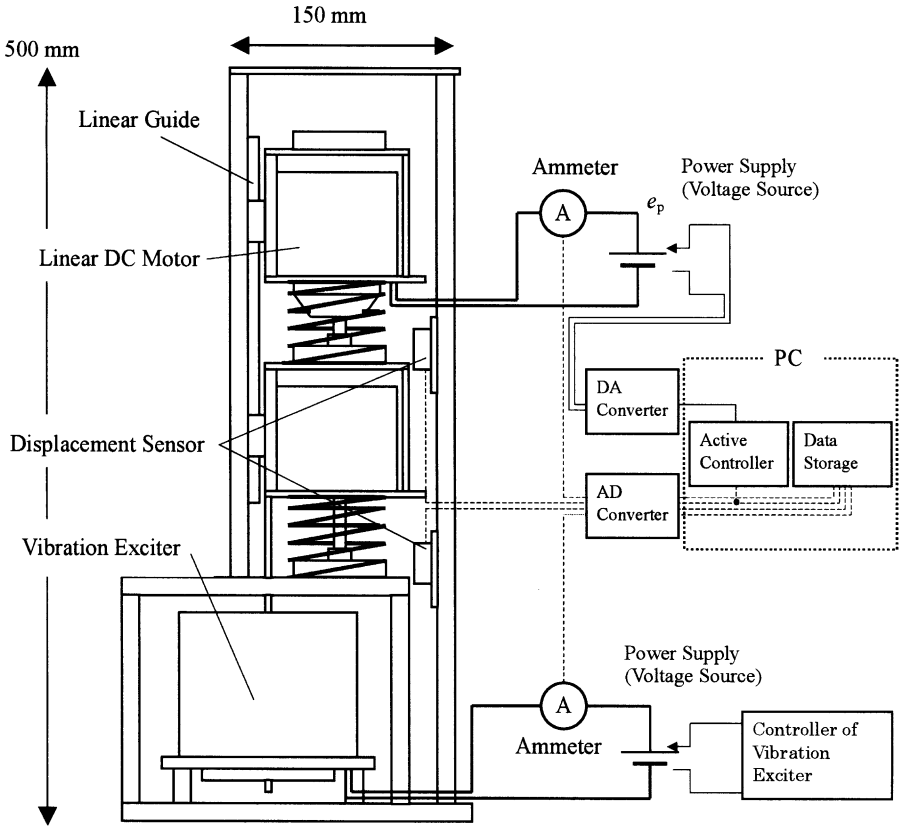

Fig. 5. Schematic view of the experimental set-up.

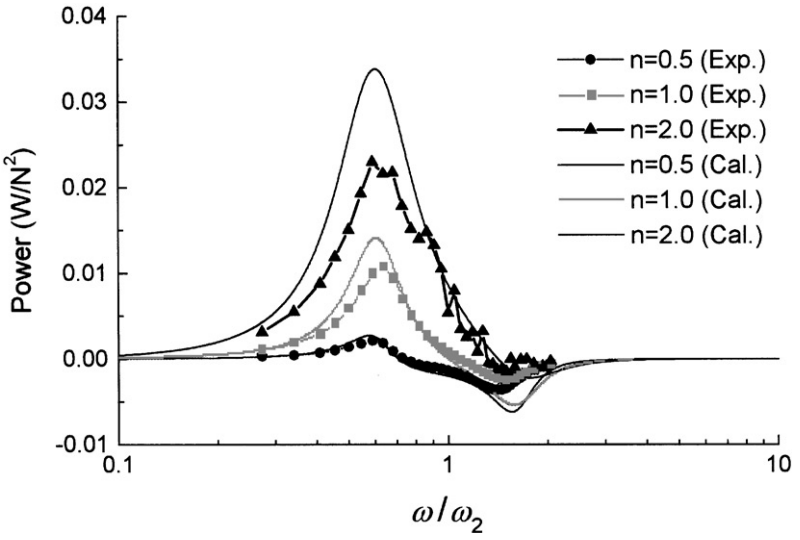

Fig. 6. Power consumption $\varepsilon_c(\omega)$.

consumption by the power spectral density of the sinusoidal force, we obtain $\varepsilon_c(\omega)$, which is defined in Eq. (23). Fig. 6 indicates $\varepsilon_c(\omega)$ when the feedback gain ratio is $n = 0.5$, 1.0 or 2.0. Normal lines and lines with symbols represent calculated values and experimental results, respectively. It is found that the experimental results show good agreement with the results of the theoretical analysis.

Power consumption when the system was subjected to random vibration was measured in the experiments. To render the results more universal, we define the following power consumption ratio:

$$\lambda = \frac{\bar{E}_c}{\bar{E}_i}, \tag{44}$$

where $\bar{E}_i$ is the average power inputted from disturbance and obtained by

$$\begin{aligned}\bar{E}_i &= \lim_{\tau\to\infty}\frac{1}{\tau}\int_0^\tau f_0\dot{x}_1\,\mathrm{d}t \\ &= \frac{1}{\pi}\int_0^\infty |G_{\dot{x}_1}(\mathrm{j}\omega)|\cos(\Phi_{\dot{x}_1}(\omega))P_0(\omega)\,\mathrm{d}\omega.\end{aligned} \tag{45}$$

Fig. 7 shows the power spectral density of the disturbance force. The spectral density is approximately constant from $\omega = 0.3\omega_2$ to $\omega = 3.0\omega_2$. The characteristic of the disturbance is similar to that of white noise. Fig. 8 indicates the power consumption when the feedback gain of the controller is equal to the equivalent damping coefficient ($n = 1$). Vertical and horizontal axes represent consumed power and time, respectively. The experiment started at 0 seconds, the average power consumption is -0.5 mW and the average power inputted from the vibration exciter is 68.0 mW. Then the non-dimensional power consumption ratio λ is –0.01, which is nearly 0.

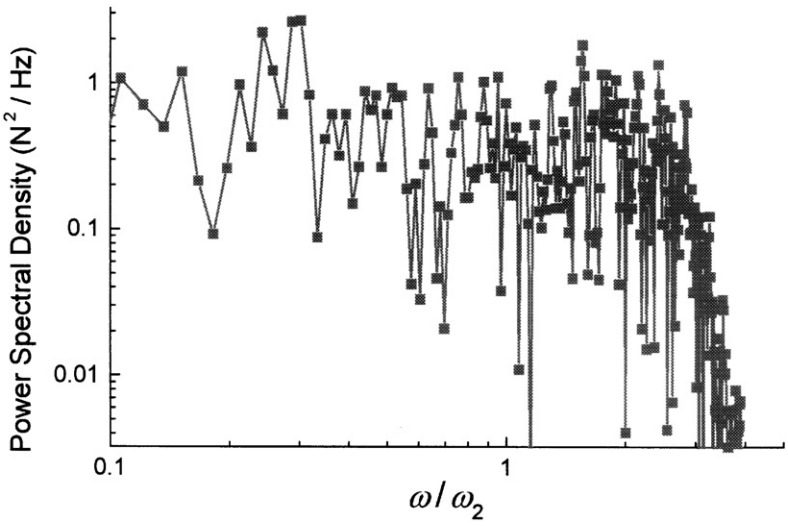

Fig. 7. Power spectral density of the disturbance.

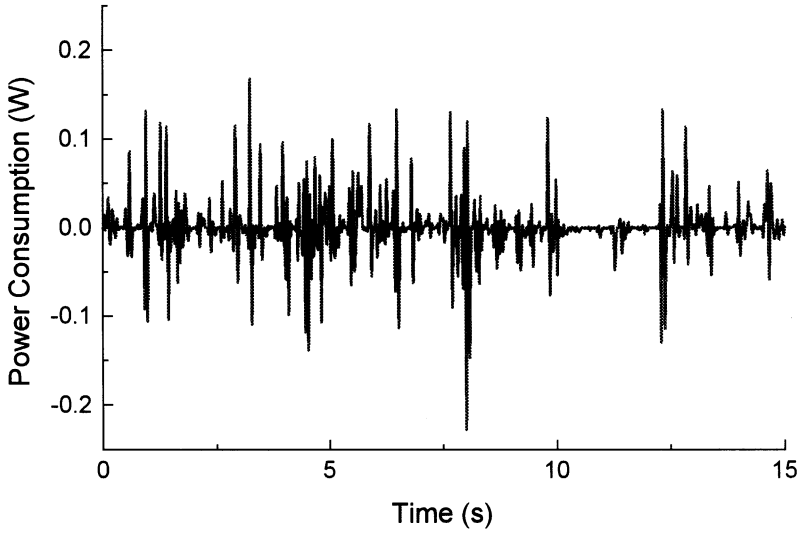

Fig. 8. Power consumption under random vibration.

4.4. Chart of energy balance

Fig. 9 shows a contour plot of the power consumption when the vibration shown in Fig. 7 is inputted. The vertical axis is the feedback gain ratio ζ_{sky}, and the lateral axis is the equivalent damping ratio ζ_{eq}. Contour lines are calculated values. Symbol marks indicate the conditions under which the experiments were carried out. The power consumption ratio is written besides the mark.

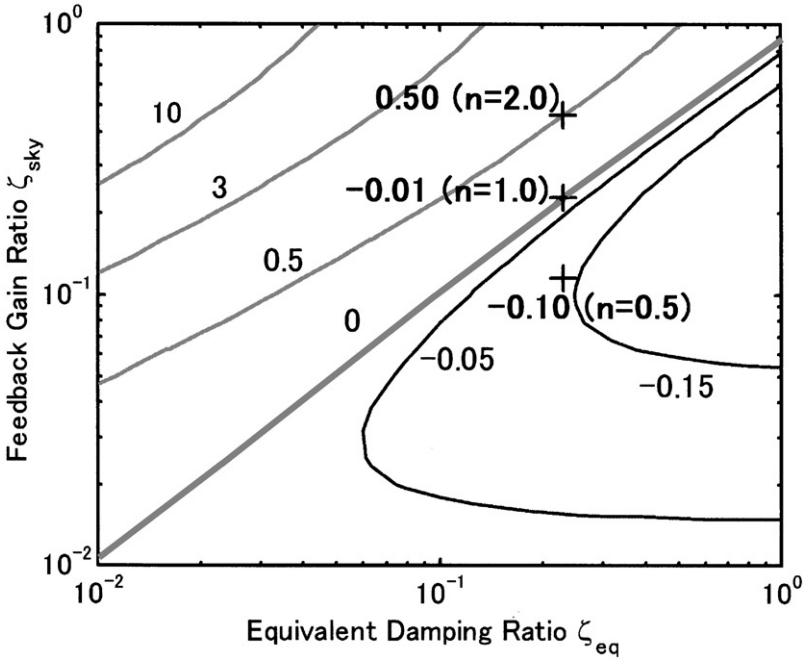

Fig. 9. Chart of power consumption: contour line represents power consumption ratio λ.

Because the disturbance utilized in the experiments was not an ideal white noise, the condition that makes the power consumption ratio negative is slightly different from the theoretical analysis presented in Section 4.2. However, the experimental results still yield good agreement with the calculated values.

From this chart, we find that the average power consumption decreases with the equivalent damping ratio and increases with the feedback gain ratio. The results indicate that the actuator with larger equivalent damping coefficient is required to realize self-powered active control that has a larger feedback gain.

5. Design of the self-powered active controller

5.1. Schematic view of the system

An area was found in which the average power consumption takes a negative value. In this area, self-powered active vibration control seemed to be attainable. However, the model used in the energy balance analysis was an ideal model. In practical systems, it is difficult to continuously control the voltage of the rechargeable power source. In this section, a control scheme to achieve self-powered active vibration control in practical systems is proposed. Fig. 10 shows the schematic view of such a system. A condenser is used as the device to accumulate energy. The circuit of the actuator includes a variable resistor in which the resistance can be controlled by a computer. This

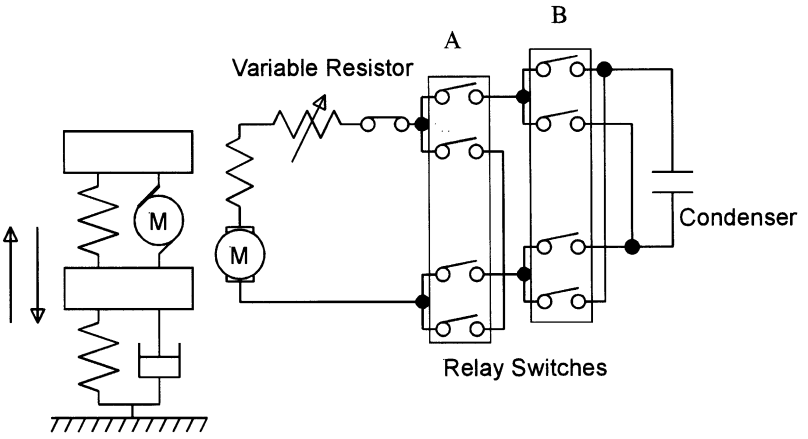

Fig. 10. Self-powered active vibration control circuit.

controls the electric current to obtain the desired motor force. Relay switches symbolized by A connect the motor to the condenser or to the shortcut circuit. Those symbolized by B change the direction of the electric current.

5.2. Control scheme

The active controller calculates the desirable control force from data measured by the displacement sensors and then decides the mode. In regeneration mode, the controller charges the condenser, while in the other modes it discharges the condenser to produce the control force. The algorithm of the self-powered active controller is shown in Fig. 11.

5.3. Regeneration mode

When $0<\gamma<1$, the actuator produces the control force with regenerating vibration energy. When the condenser voltage is e_c and resistance of the variable resistor is r_{var}, output of the actuator is

$$f = \varphi\frac{(\sigma e_c - \varphi\dot{z})}{r + r_{var}}. \tag{46}$$

It is found that resistance r_{var} that realizes the desirable force f^* is

$$r_{var} = \left|\frac{\varphi}{f^*}(\sigma e_c - \varphi\dot{z})\right| - r, \tag{47}$$

where

$$\begin{aligned} \sigma &= 1 \quad (\dot{z}\geqslant 0), \\ \sigma &= -1 \quad (\dot{z}<0). \end{aligned} \tag{48}$$

When $|\varphi(\sigma e_c - \varphi\dot{z})| - |f^*|r<0$, the actuator cannot produce the desired force. In this mode, the actuator halts regenerating energy. As it is connected to the shortcut circuit, it acts as a viscous

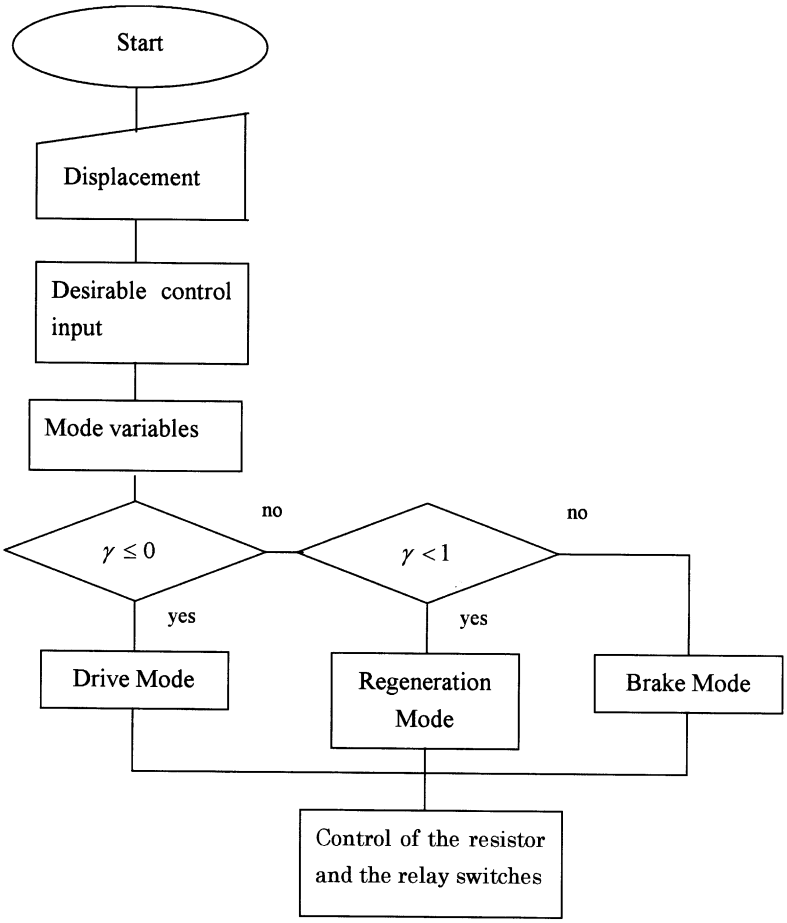

Fig. 11. Algorithm of self-powered active controller.

damper, and by controlling the variable resistor it produces the desired force. Output of the actuator is

$$f = \varphi \frac{-\varphi \dot{z}}{r + r_{var}}. \tag{49}$$

Resistance r_{var} is decided as

$$r_{var} = \left| \frac{-\varphi^2}{f^*} \dot{z} \right| - r. \tag{50}$$

Fig. 12 shows the electric circuit when $0 < \gamma < 1$ and $(|\varphi(\sigma e_c - \varphi \dot{z})| - |f^*|r) \geqslant 0$, and Fig. 13 shows one when $0 < \gamma < 1$ and $(|\varphi(\sigma e_c - \varphi \dot{z})| - |f^*|r) < 0$. The circuits presented in Fig. 12 are when $\dot{z} > 0$. When $\dot{z} \leqslant 0$, the actuator is connected to the condenser in the opposite direction.

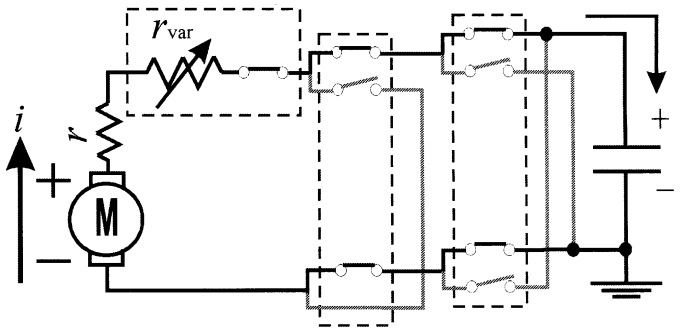

Fig. 12. Circuit in regeneration mode when $|\varphi(\sigma e_c - \varphi\dot{z})| - |f^*|r \geqslant 0$.

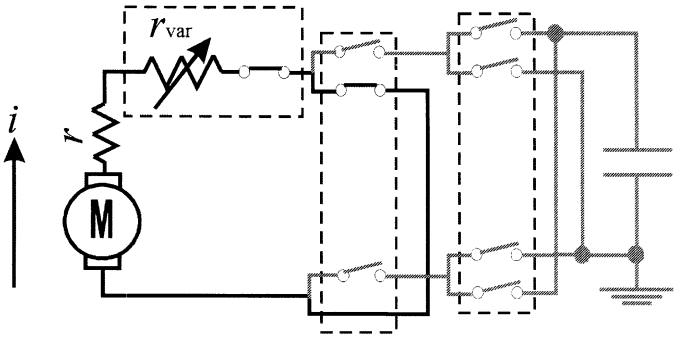

Fig. 13. Circuit in regeneration mode when $|\varphi(\sigma e_c - \varphi\dot{z})| - |f^*|r < 0$.

5.4. Drive mode

When $0 \geqslant \gamma$, the actuator produces a negative damping force using energy stored in the condenser. Output of the actuator is

$$f = \varphi\frac{(\sigma e_c - \varphi\dot{z})}{r + r_{var}}. \tag{51}$$

Resistance r_{var} is obtained by

$$r_{var} = \left|\frac{\varphi}{f^*}(\sigma e_c - \varphi\dot{z})\right| - r \tag{52}$$

When r_{var} becomes less than zero, the resistance of the resistor is assigned to be zero and the system cannot produce the desired force. Furthermore, when $e_c < \varphi|\dot{z}|$, the electric current flows from the actuator to the condenser. To prevent this counter current, the actuator is insulated from the condenser. In this mode, the actuator produces no force. Figs. 14 and 15 show the circuit when $0 \geqslant \gamma$ and $e_c \geqslant \varphi|\dot{z}|$ and that when $0 \geqslant \gamma$ and $e_c < \varphi|\dot{z}|$, respectively.

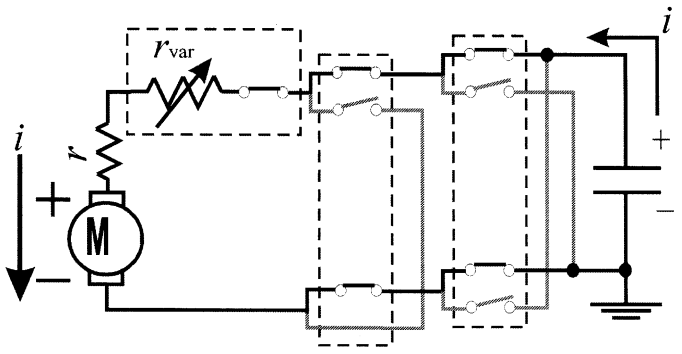

Fig. 14. Circuit in drive mode when $e_c \geqslant \varphi|\dot{z}|$.

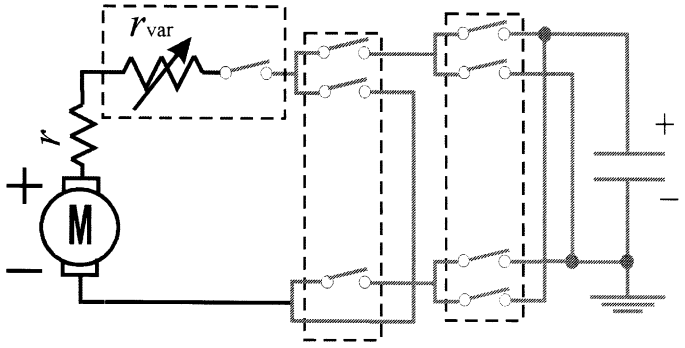

Fig. 15. Circuit in drive mode when $e_c < \varphi|\dot{z}|$.

5.5. Brake mode

In the case of $1 \leqslant \gamma$, the actuator increases its damping force using the energy accumulated in the condenser. Output of the actuator is written as

$$f = \varphi \frac{(-\sigma e_c - \varphi \dot{z})}{r + r_{var}}. \tag{53}$$

Resistance of the variable resistor is decided as

$$r_{var} = \left| \frac{\varphi}{f^*}(-\sigma e_c - \varphi \dot{z}) \right| - r \tag{54}$$

When resistance r_{var} is less than zero, r_{var} is assigned to be zero. In this case, the actuator cannot produce the desired force.

In brake mode, the system has a chance to apply reverse voltage to the condenser. When a polar-type condenser is utilized, this should be avoided. The threshold of the condenser voltage, e_{min}, is then decided, and when it is lower than the threshold, the actuator is connected to the shortcut circuit. Resistance of the resistor is kept at a minimum value, that is, zero. Output of the

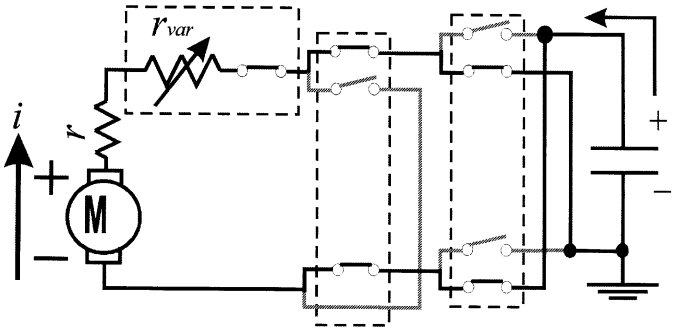

Fig. 16. Circuit in brake mode when $e_c \geqslant e_{min}$.

actuator is

$$f = \varphi \frac{-\varphi \dot{z}}{r}. \tag{55}$$

In this case the output is not identical to the desired value.

Fig. 16 shows the circuit when $1 \leqslant \gamma$ and $e_c \geqslant e_{min}$. When $e_c < e_{min}$, the circuit is same as shown in Fig. 13.

6. Self-powered active vibration control performance

6.1. Laboratory test

Self-powered active vibration performance was examined in experiments. The experimental set-up is the same as utilized in the energy balance analysis shown in Fig. 5, except for the electric circuit attached to the linear DC motor, which is shown in Fig. 10. The capacity of the condenser is 0.044 F. The variable resistor takes 15 different values: 0.0, 2.3, 6.2, 12.1, 18.3, 24.7, 36.9, 48.5, 61.2, 73.8, 98.3, 123.5, 181.9, 295.7, and 622.3 Ω. Furthermore the resistor can insulate the circuit and the computer can change these values in real-time.

The laboratory test was carried out for 15 s. The vibration shown in Fig. 7 was utilized as the disturbance. The feedback gain of the skyhook controller was $0.8c_{eq}$, since the energy balance analysis estimated power consumption to be less than zero. Fig. 17 shows the output of the actuator and its desired force. It can be seen that the actuator force follows the desired force well, indicating that self-powered active vibration control has been reached.

6.2. Condenser voltage

Fig. 18 shows the condenser voltage. Initial voltage was 0 V. After the self-powered active vibration control started, it rose with fluctuations and reached 0.14 V at 15 s. The fluctuations occurred because the three modes changed alternately.

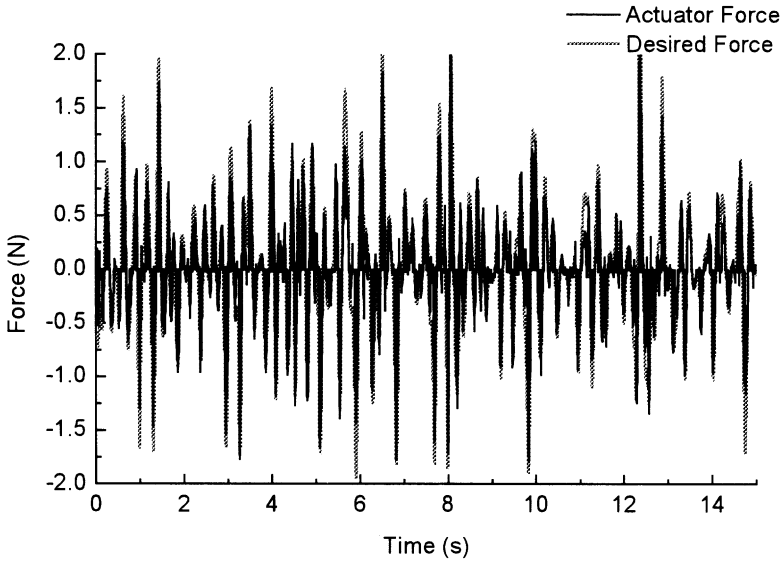

Fig. 17. Actuator force compared with desirable force.

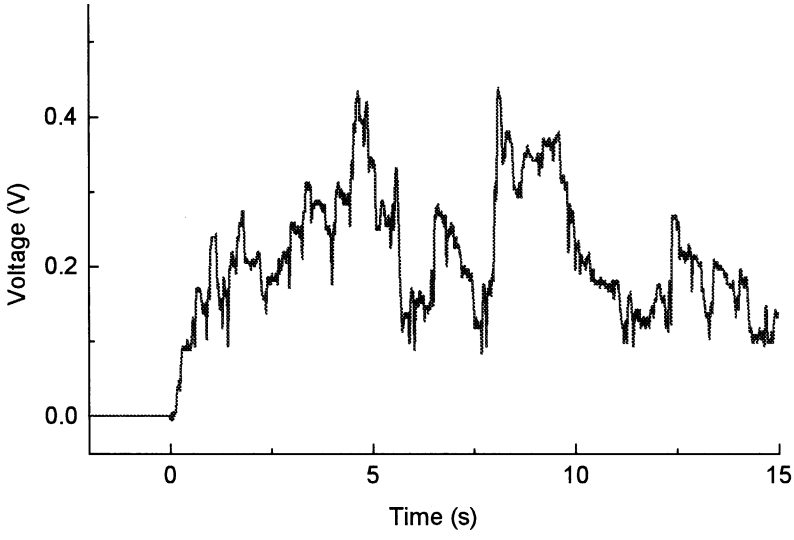

Fig. 18. Condenser voltage.

6.3. Suppression performance

Transmissibility of the second mass displacement from the disturbance was obtained from the experimental results. It was derived by

$$|G_{x_2}(\mathrm{j}\omega)| = \sqrt{\frac{P_{x_2}(\omega)}{P_0(\omega)}}. \tag{56}$$

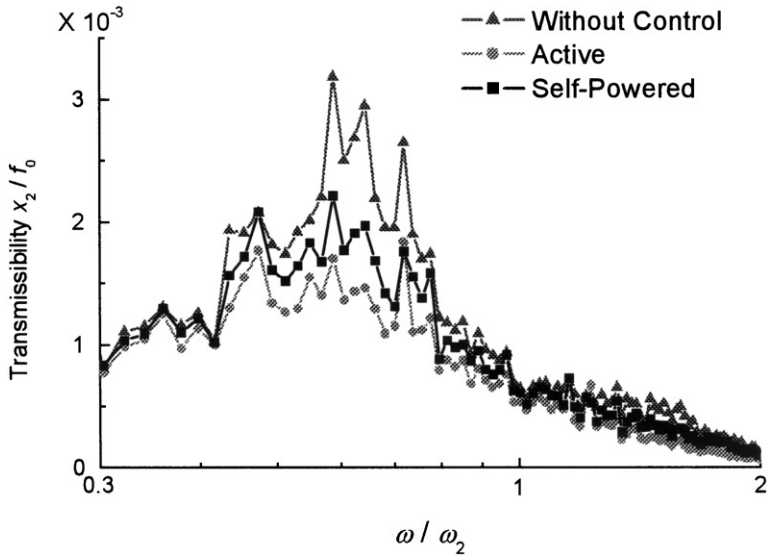

Fig. 19. Transmissibility of the proposed system compared with systems with or without active control.

Fig. 19 shows transmissibilities of the self-powered active control system, an active control system using the external power source, and a system without control. Although performance of the proposed system is slightly inferior to that of the active control with external power, it has a better isolation performance than a system without control.

7. Discussion

Fig. 20 shows the actuator force along with the desired force when $n = 0.5$. The actuator force follows the desired force well. The actuator force and the desired force, when $n = 2.0$, are shown in Fig. 21. It is clear that the actuator force cannot follow the desired force. The system with $n = 0.5$ is in an area where the average power consumption is less than zero, while the average power consumption of the system with $n = 2.0$ is greater than zero (Fig. 9); the result validates our claim that a self-powered active vibration controller should be designed based on an energy balance analysis.

8. Conclusions

(1) The proposed energy balance analysis predicting the feasibility of self-powered active vibration control was validated by the experimental results.
(2) A practical system to produce control force with regenerating vibration energy was proposed.
(3) The experimental results indicated that the proposed system could be achieved under suitable conditions derived from the energy balance analysis.
(4) The procedures to design a self-powered active control were set out.

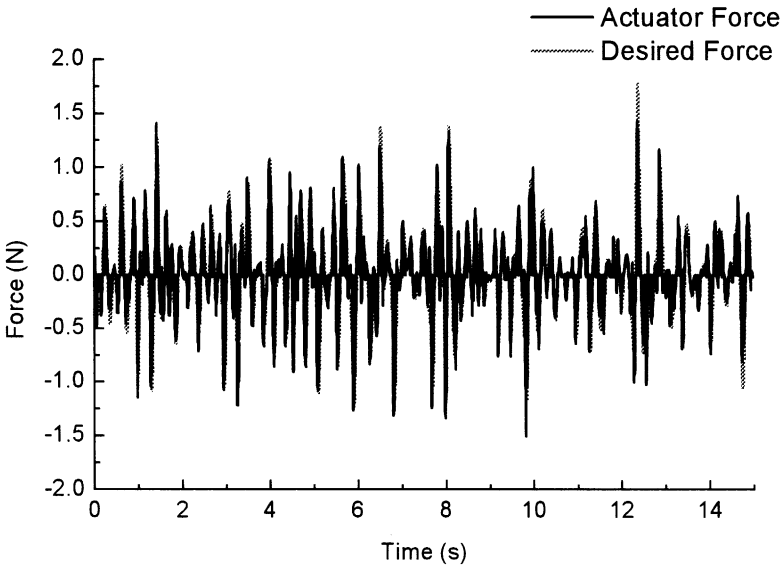

Fig. 20. Actuator force compared with the desired force ($n = 0.5$).

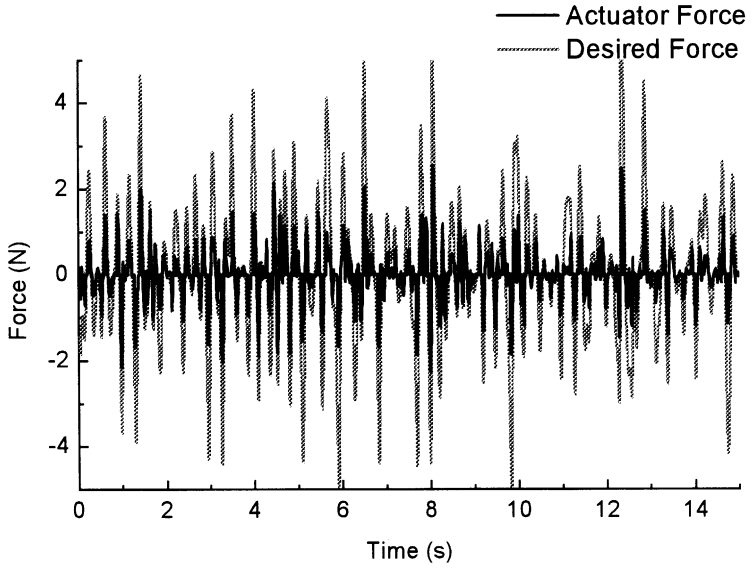

Fig. 21. Actuator force compared with the desired force ($n = 2.0$).

Acknowledgements

The authors would like to express their thanks to The Ministry of Education, Culture, Sports, Science and Technology of Japan for financial support through a Grant-in-Aid for Scientific Research.

Appendix A. Nomenclature

c	capacity of condenser
c_1	damping constant
c_{eq}	equivalent damping coefficient
c_{sky}	feedback gain of skyhook controller
e_p	voltage of power source
e_i	induced voltage
E_c	power consumption
$\bar{E}_c$	average power consumption
$\bar{E}_i$	average power inputted from disturbance
f	actuator force (control input)
f_0	disturbance
f^*	desired actuator force
G_{f_a}	transfer function of control input to disturbance
$G_{\dot{x}_1}$	transfer function of velocity of primary mass to disturbance
$G_{\dot{z}}$	transfer function of stroke velocity to disturbance
i	electric current
j	imaginary number ($j^2 = -1$)
k_1	spring constant of primary suspension
k_2	spring constant of secondary suspension
m_1	primary mass
m_2	secondary mass
M_c	actuator output power
n	feedback gain ratio
P_0	power spectral density of disturbance
P_{x_2}	power spectral density of second mass displacement
r	resistance of armature
r_{var}	resistance of variable resistor
x_1	displacement of primary mass
x_2	displacement of secondary mass
z	stroke of actuator
γ	mode variable
λ	power consumption ratio
Φ_f	phase angle of control input
$\Phi_{\dot{x}_1}$	phase angle of primary mass velocity
$\Phi_{\dot{z}}$	phase angle of stroke velocity
φ	motor constant
ω	angular frequency
ω'	non-dimensional angular frequency
ω_1	natural frequency of primary suspension
ω_2	natural frequency of secondary suspension
ζ_1	damping ratio of primary suspension

ζ_{eq} equivalent damping ratio
ζ_{sky} feedback gain ratio

References

[1] D. Karnopp, G. Heess, Electronically controllable vehicle suspensions, Vehicle System Dynamics 20 (1991) 207–217.
[2] L. Segal, L. Xiao-Pei, Vehicular resistance to motion as influenced by road roughness and highway alignment, Australian Road Research 12 (4) (1982) 211–222.
[3] M.G. Fodor, R. Redfield, The variable linear transmission for regenerative damping in vehicle suspension control, Vehicle System Dynamics 22 (1993) 1–20.
[4] Y. Suda, T. Shiiba, Study on vibration control with energy regenerative System, Proceeding of the Sixth Symposium on Electromagnetics and Dynamics, JSME 940–26, 1994, pp. 483–488 (in Japanese).
[5] Y. Suda, T. Shiiba, A new hybrid suspension system with active control and energy regeneration, Vehicle System Dynamics Supplement 25 (1995) 641–654.
[6] Y. Suda, S. Nakadai, K. Nakano, Hybrid suspension system with skyhook control and energy regeneration (development of self-powered active suspension), Vehicle System Dynamics Supplement 28 (1998) 619–634.
[7] K. Nakano, Y. Suda, S. Nakadai, Self-powered active vibration control using continuous control input, JSME International Journal Series C 43 (3) (2000) 726–731.
[8] K. Nakano, Y. Suda, S. Nakadai, Self-powered active vibration control with continuous control input (application to a cab suspension of a heavy duty truck). Proceedings of DETC'99 ASME Design Engineering Technical Conferences, DETC99/MOVIC-8404, 1999.
[9] G.R. Wendel, G.L. Stecklein, A regenerative active suspension system, SAE Publication SP-861, Paper No. 910659, 1991, pp. 129–135.
[10] T. Saito, Y. Sumino, S. Kawano, Research on energy conversion of mechanical vibration (in Japanese), Proceedings of the Dynamics and Design Conference '93 (Vol. B), JSME 930–42, 1993, pp. 105–108.
[11] H. Harada, Y. Okada, K. Suzuki, Active and regenerative control of an electrodynamic-type suspension (in Japanese), Transactions of the Japan Society of Mechanical Engineers 62 (604) (1995) 4513–4519.
[12] S. Kim, Y. Okada, Energy regenerative damper using pulse width modulated (PWM) step-up chopper, Proceedings of DETC'99 ASME Design Engineering Technical Conferences, DETC99/MOVIC-8415, 1999.
[13] N. Noritsugu, O. Fujita, S. Takehara, Control and energy regeneration of active air suspension (in Japanese), Proceedings of the Dynamics and Design Conference '96 (Vol. A), 1996, pp. 227–230.
[14] M.R. Jolly, D.L. Margolis, Regenerative systems for vibration control, Transactions of the American Society of Mechanical Engineers, Journal of Vibration and Acoustics 119 (1997) 208–215.
[15] D. Karnopp, M.J. Crosby, R.A. Harwood, Vibration control using semi-active force generators, Transactions of the American Society of Mechanical Engineers, Journal of Engineering for Industry 96 (1974) 619–626.
[16] R. Davor, L. Jezequel, J.C. Sauvageot, Analysis of the procedures of active control of vehicle suspensions and of their strength, Proceedings of the 18th FISITA Congress, SAE, 1990, pp. 47–57.
[17] D. Karnopp, Minimum energy-loss control of electro- and hydro-mechanical modulated converter drives, Transactions of the American Society of Mechanical Engineers, Journal of Mechanical Design 103 (1981) 48–53.
[18] B. Seth, W.C. Flowers, Generalized actuator concept for the study of the efficiency of energetic systems, Transactions of the American Society of Mechanical Engineers, Journal of Dynamic, Systems, Measurement and Control 112 (1981) 233–238.